Molecular balances for quantifying non-covalent interactions

Post-print of a peer-reviewed article published by the Royal Society of Chemistry.
Published article available at: http://dx.doi.org/10.1039/B822665M

Cite as:
Mati, I. K., & Cockroft, S. L. (2010). Molecular balances for quantifying non-covalent interactions. *Chemical Society Reviews*, 39(11), 4195-205.

Manuscript received: 12/04/2010; Article published: 16/09/2010

Molecular balances for quantifying non-covalent interactions**

Ioulia K. Mati and Scott L. Cockroft*

EaStCHEM, School of Chemistry, Joseph Black Building, University of Edinburgh, West Mains Road, Edinburgh, EH9 3JJ, UK.

[*]Corresponding author; e-mail: scott.cockroft@ed.ac.uk, tel: +44 (0)131 650 4758

[**]We thank Dr. John Brazier for helpful discussions, and the EPSRC and the School of Chemistry at the University of Edinburgh for a PhD scholarship to I. K. M.

Graphical abstract:

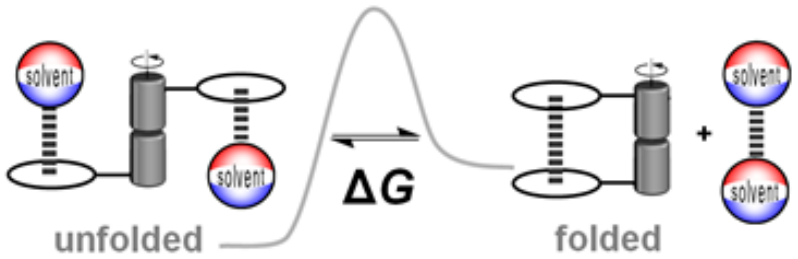

Summary:
Folding molecules provide an attractive platform for the quantitative study of non-covalent interactions in solution.

Abstract

Molecular interactions underlie the whole of chemistry and biology. This tutorial review illustrates the use of rotameric folding molecules, topoisomers, atropoisomers, and tautomers as molecular balances for quantifying non-covalent interactions. This intramolecular approach enables a wide variety of interactions to be examined with a degree of geometric control that is difficult to achieve in supramolecular complexes. Synthetic variation of molecular balances allows the fundamental physicochemical origins of molecular recognition to be systematically examined by providing insights into the interplay of geometry and solvation on non-covalent interactions.

1. Introduction

Non-covalent interactions are fundamental aspects of all chemical and biological processes. In the chemical sciences, non-covalent interactions have essential roles in template-directed synthesis,[1] the transmission of stereochemical information,[2] and in determining the structure and properties of materials.[3] Meanwhile, in biological systems, non-covalent interactions govern the secondary and tertiary structure of proteins,[4] and are responsible for enzyme-ligand binding and base-pairing in nucleic acids.[5]

Detailed study of non-covalent interactions in biological systems is often complicated by arrays of interactions featuring multiple molecular contacts and solvent molecules. Furthermore, the precise geometry of an interaction of interest is hard to determine in conformationally-dynamic biomolecules. Such complexities can be side-stepped by using minimal synthetic compounds in the study of non-covalent interactions.[6] Synthetic chemistry facilitates the design of molecules that allow the systematic study of the underlying phenomena that determine the strength of non-covalent interactions. Whilst non-covalent interactions have been examined extensively using supramolecular complexes,[7] unimolecular approaches often offer improved control over the geometry of an intramolecular interaction of interest, which is a major advantage since small alterations in geometry may have a considerable effect on the strength of an interaction. Furthermore, very weak interactions that are too weak to overcome the entropic penalty associated with intermolecular association, or that would otherwise provide only a minor perturbation to the overal stability of an intermolecular complex can often be measured accurately using molecular balances.

2. Quantifying Non-covalent Interactions with Molecular Balances

Folding molecules offer an attractive platform for the study of non-covalent interactions, since the relative stabilities of the conformational states are governed by intramolecular contacts and solvent

interactions that are present in one conformation, but absent in the others. Although it is not possible to experimentally assess the relative stabilities of all accessible conformations of a flexible molecule, thermodynamic information can be extracted from simple model systems with limited degrees of conformational freedom. The most elegant molecular torsion balances possess high degrees of symmetry, which minimises the contributions of background steric, solvent and secondary intramolecular interactions to the folding behaviour of the molecule. When the system lacks symmetry or when changing functional groups perturbs multiple interactions in the system, then the interaction of interest can be dissected from the background secondary effects by reference to suitable control compounds and application of thermodynamic double-mutant cycles.[15]

Though not all molecules have the desired folding properties to permit ΔG determination, numerous molecular systems have been successfully applied to the quantitative study of non-covalent interactions. Rotational barriers ($\Delta G^{\ddagger}$) and differences in the free energies of ground-state conformers (ΔG) are used most frequently to assess the thermodynamics of non-covalent interactions.

$\Delta G^{\ddagger}$ Rotational barrier measurement - theoretical requirements & limitations

The barrier to rotation about a single covalent bond ($\Delta G^{\ddagger}$) quantifies the free energy difference between a ground-state conformation and the transition state, and can provide insight into the strength of non-covalent interactions (Figure 1). Although $\Delta G^{\ddagger}$ values can be readily determined using variable-temperature dynamic NMR spectroscopy, the interpretation of these measurements is not always straightforward since the nature of the transition state can be hard to define.[8] The conformation of the transition state cannot be observed directly, and the energetic effects of substituents on the stability and the structure of highly strained or sterically crowded transition states can be particularly difficult to predict.

ΔG Conformational equilibrium measurement - theoretical requirements & limitations

The free energy difference between ground-state conformers (ΔG) is more easily interpreted than $\Delta G^{\ddagger}$ rotational barrier measurements because the interactions present in the ground-state conformations can often be calculated with a high degree of certainty or observed experimentally (*i.e.* in X-ray crystal structures or NMR solution structures). However, interaction energies should always be interpreted with care; the role of the solvent in determining molecular conformation should never be overlooked (Figure 1).[9-12]

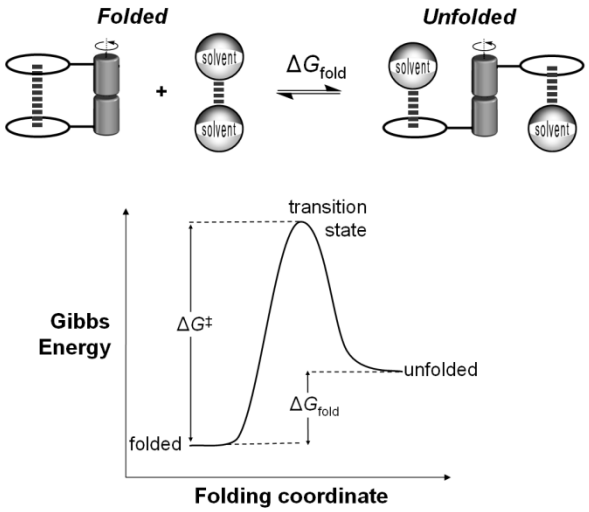

← ***Figure 1.*** Simplified folding equilibrium for a molecular torsion balance including the solvent and the corresponding energy profile showing the energy barrier to rotation, $\Delta G^{\ddagger}$ and the free energy of folding, ΔG_{fold}. In this example, folding involves the formation of an intramolecular interaction accompanied by desolvation of the interacting functional groups.

The foremost requirement for ΔG measurement using folding molecules is that the relative populations of each distinct conformer must be quantifiable. NMR spectroscopy is a powerful technique for assessing the conformation of small molecules. However, it is not always possible to quantify folding equilibria because most forms of molecular flexibility are rapid on the NMR timescale and result in conformationally averaged signals. Thus, not all folding molecules are suited to the quantitative study of non-covalent interactions. For example, the folding compounds depicted in Figure 2 have been used to investigate aromatic stacking interactions.[13, 14] Qualitative information about the preferred geometry of these molecules can be obtained from spectroscopic techniques, but thermodynamic information cannot be extracted from the system because the precise position of the conformational equilibrium cannot be determined.

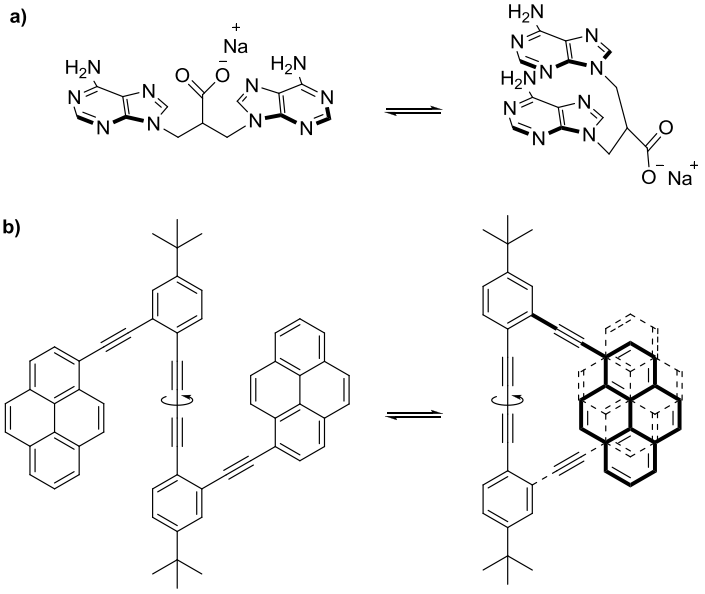

← ***Figure 2.*** Folding molecules synthesised by a) Gellman,[13] and b) Sankararaman for studying aromatic interactions.[14] Despite the elegant, simplistic designs, neither system can be used to quantify the interaction of interest as no method of accurately determining the position of the equilibrium has been established.

One approach to quantifying ground-state non-covalent interactions is to exploit molecules featuring a single restricted bond that rotates slowly enough for distinct conformational populations to be directly quantified by NMR, but rapidly enough for conformational equilibrium to be reached within a reasonable timescale. For room-temperature analysis using ^{1}H NMR this typically requires a barrier to rotation, $\Delta G^{\ddagger} > 65$ kJ mol^{-1}. Integration of distinct NMR conformer signals allows the conformational equilibrium constant K_{fold} to be determined from a single NMR spectrum. One advantage of this approach is that time-consuming titrations, or variable-temperature experiments are not required to extract thermodynamic information from the system. Provided that the system under investigation is sufficiently geometrically well-defined, the approach allows both attractive and repulsive interactions to be measured with a high degree of accuracy (often ±0.5 kJ mol^{-1}). The precise range and accuracy of the approach depends upon the sensitivity of the spectroscopic technique employed. For example, ^{1}H-NMR spectra with an integral accuracy ~5% provides an interaction window of 14.6 kJ mol^{-1} since the most extreme conformational populations that can be measured accurately correspond to $\Delta G_{fold} = -RT \ln K_{fold} = RT \ln(5/95) = +7.3$ kJ mol^{-1} and $\Delta G_{fold} = -RT \ln(95/5) = -7.3$ kJ mol^{-1}.

3. Classes of interaction investigated using molecular balances

3.1 CH···O Interactions

Ōki's pioneering studies of restricted bond rotation in triptycene derivatives date back to the 1970s. Ōki was quick to realise that interactions between substituents in the 1-(*peri*) and 9-(bridge-head) positions influenced the rotational barrier about the C-C bond indicated in Figure 3.[16] Furthermore, when the substituents in these positions were large enough, the increased barrier to rotation meant that distinct conformers could be observed in ^{1}H-NMR spectra at low temperatures.[18] The substituents attached to the 1- and 9- positions are able to interact with each other in the folded ±*syn* conformation, whilst they are splayed apart in the unfolded *anti* conformation. Based on the equilibrium shown in Figure 3, the magnitude of the intramolecular interaction between the 1- and 9- substituents (including steric and solvophobic effects) can be determined by measuring the deviation from the statistically expected ±*syn*/*anti* ratio of 2:1.[16] Ōki went on to study many types of non-covalent interactions using triptycene balances,[17] and some of these findings are summarised below and interpreted from a contemporary point of view.[19]

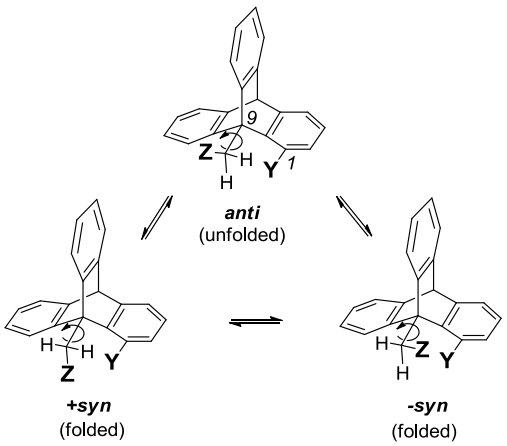

Figure 3. Conformational equilibrium in 1,9-disubstituted triptycenes.[16, 17]

A series of triptycene torsion balances was synthesised to study the interactions of methoxy groups with a range of functional groups in $CDCl_3$ (Figure 4a).[20-22] In general, the folded ±*syn* conformers were most favoured when the R-groups were electron-withdrawing, which was consistent with an electrostatically dominated interaction between the electron-rich oxygen and the δ+ CH_2 groups adjacent to the carbonyl group.[21] There were a few exceptions to this rule that were attributed to conformational and steric differences related to the positioning of the functional groups as the R-group was varied.[20, 22] When the methoxy group was replaced with a chlorine atom, the ±*syn*/*anti* ratios decreased due to the increased size and decreased electron density of chlorine compared to oxygen. Two different families of torsion balances were then synthesised to investigate CH···O interactions (Figs. 4a bottom, R = H and 4b).[23, 24] In both series, the unfolded *anti* conformer was always favoured, which was attributed to the dominance of van der Waals repulsion over the electrostatic CH···O interactions. Consistent with the presence of a favourable CH···O non-covalent interaction, the population of the folded *syn* conformer increased as the oxygen atom became more electron-rich for the compounds depicted in Figure 4b. In contrast, the population of the unfolded *anti* conformer increased as the X-substituent became more electron donating for the other compound series (R = H, Figure 4a).[24] This inconsistency was reasoned as being due to the increased polarity of the benzyl CH *vs.* ethyl CH, although modern-day electrostatic surface potential calculations show that these functional groups have only a marginal difference in polarity (+49 kJ mol^{-1} for the toluene CH_3 *cf.* +43 kJ mol^{-1} for the CH_3 in ethyl benzene at DFT/B3LYP/6-31G*). Further insight into this discrepancy can be gained from examination of molecular models (Figure 5). Space-filling models indicate that the ethyl group occludes most of the methoxy oxygen in the folded *syn* conformation, whereas the phenolic oxygen in the other compound series remains accessible to solvation by chloroform in the *syn* conformation. Since chloroform is a stronger H-bond donor (α = 2.2) than an alkyl group (α = 0.4) solvation of the methoxy group by chloroform outcompetes the Et···O interaction.[19] Thus, the steric occlusion of the methoxy oxygen in the folded *syn* conformer means that desolvation

dominates the population ratios for the compound series where R = H (Figure 4a), whilst the phenolic compounds (Figure 4b) are much less affected by desolvation and the CH···O interaction governs the folding behaviour as the Y-substituents are varied. These experiments highlight the subtle interplay of geometry and the effects of desolvation on non-covalent interactions.

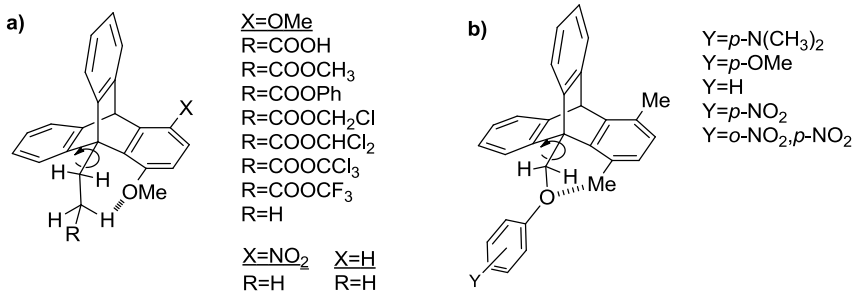

Figure 4. 1,9-disubstituted triptycenes for investigating CH···O interactions in $CDCl_3$. a) The folded *syn* conformer (depicted) becomes more prevalent as the R-group becomes more electron-withdrawing, which is consistent with the presence of a polar CH···O interaction. However when R = H, steric and desolvation effects dominate and the unfolded *anti* conformer is favoured (Figure 5a).[20-22, 24] b) The folded *syn* conformer depicted is most favoured when the phenolic Y-substituents are electron donating.[23]

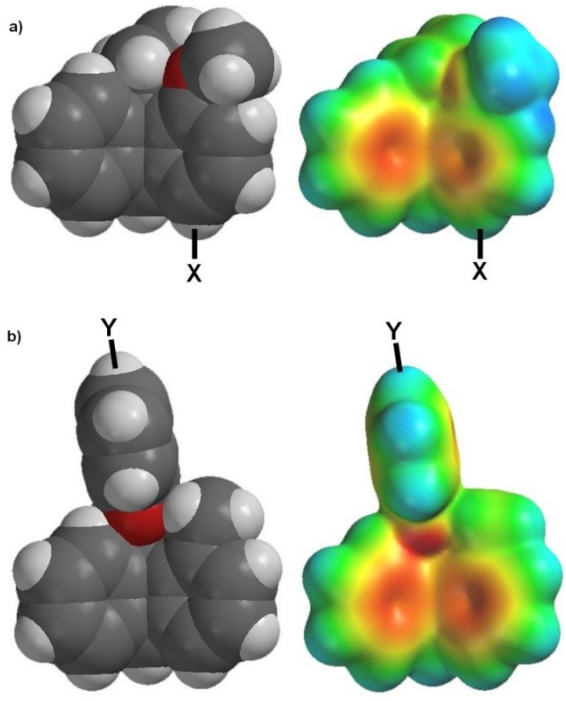

← ***Figure 5.*** Space-filling models (left) and electrostatic surface potentials (right) of triptycene balances minimised at the DFT/B3LYP/6-31G* level. Electrostatic potentials are scaled from –115 kJ mol^{-1} (red) to +115 kJ mol^{-1} (blue); green corresponds to neutral charge. a) The negative charge on the oxygen atom is solvent-occluded in the *syn* conformer of the ethyl balance shown (Figure 4a, R = H), but solvent exposed in the *anti* conformation (not shown). Thus, the trend in the folding behaviour as the X-substituent is varied is dominated by the effects of chloroform desolvation. b) In contrast, the electron density of the oxygen atom is not sterically occluded in the *syn* conformer of the phenoxy balance and can be freely solvated by the polar C-H of chloroform (Figure 4b). As a result the trends in the folding behaviour of the phenoxy balance are governed by the strength of the CH···O interaction as the Y-substituents are varied rather than by the effects of desolvation.

3.2 Arene···functional-group interactions

Building on his earlier studies of CH···O interactions, Ōki and more recently, Gung, have synthesised a series of 9-benzyl triptycene derivatives for investigating arene···functional group interactions (Figure 6). The compounds shown in Figure 6a were synthesised for studying CH_3···arene interactions as the X and Z substituents were varied.[17] Chlorine atoms were used in two of the *peri*-positions in this compound series to approximately balance the influence of steric effects on the *syn*/*anti* conformer ratio (Cl has a similar van der Waals radius to Me). Thus, the position of the folding equilibrium should be mostly determined by the relative energies of the Cl/CH_3···arene interactions and desolvation effects. Consistent with the formation of a dominant CH···arene interaction, higher ±*syn*/*anti* ratios were observed for the compounds with the most electron-rich aromatic ring (Z = NMe_2) and the most positively polarised CH_3-group (X = $COOCH_3$).

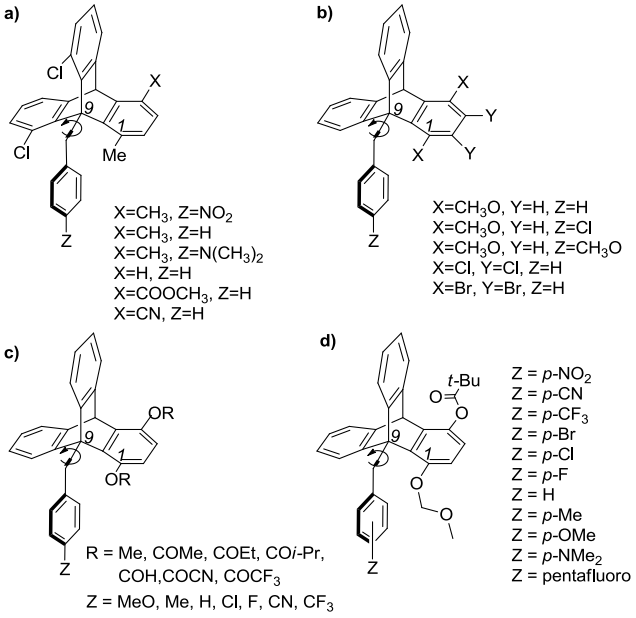

Figure 6. 9-Benzyl triptycene derivatives for investigating functional group···arene interactions. a) and b) Ōki's compounds for studying CH···arene and oxygen/halogen···arene interactions.[17] c) and d) Gung's systems for studying oxygen···arene interactions,[24] and methoxymethyl···arene interactions.[26]

Oxygen···arene and halogen···arene interactions were studied using the compounds shown in Figure 6b.[17] Introduction of electron-donating Z-substituents was seen to decrease the *syn/anti* ratio, and this was attributed to the increase in electrostatic repulsion between the oxygen atom and the face of the aromatic ring. The *syn/anti* ratio was reduced when the X-substituents were replaced with larger chlorine or bromine atoms.

Gung and co-workers have investigated interactions between aromatic rings and a series of esters (Figure 6c)[25] and methoxymethyl ether groups (Figure 6d).[26] There was a preference for the folded *syn* conformer in almost all cases. The greatest preference for the folded conformation was observed in the methoxymethyl ether series (Figure 6d), particularly when the arene contained electron-withdrawing Z-substituents. Interpretation of these data may be complicated by the conformational freedom of the functional groups studied, which permits multipoint contacts of both positively polarised CH-groups and electron-rich oxygen atoms with the rotameric phenyl ring. Although the role of the solvent on these conformational equilibria has yet to be systematically examined, the authors suggest that the preference for the folded state points towards the importance of van der Waals dispersion forces, with the position of the equilibrium being modulated by electrostatic interactions.

Motherwell and co-workers have used minimal dibenzobicyclo[3,2,2]-nonane derivatives to study interactions between functional groups and aromatic rings (Figure 7).[27, 28] These compounds exist in two conformations, where either the Y or Z group interacts with the face of an aromatic ring. In contrast to many of the other folding molecules presented in this review, the barrier to isomerisation in these derivatives is small and the rate of the conformational interconversion is not slow on the NMR timescale. Nevertheless, accurate population ratios were determined from the ^{1}H-NMR *J*-couplings of the conformers.[27] When Y = Me and Z = OH, the conformation in which the hydroxyl group interacts with the aromatic ring is observed in the solid-state and also dominates in low polarity solvents such as cyclohexane, carbon tetrachloride, benzene, toluene and chloroform (population of *D* >89%). Meanwhile, solvents that act as H-bond acceptors, such as pyridine, methanol, and dimethylsufoxide ($\beta_s \approx$ 6-9) compete with the OH···arene interaction and the equilibrium is shifted towards the *U* conformation (population of *D* = 50-55%). Acetronitrile competes less strongly with the OH···arene interaction (population of *D* = 74%) since it is a weaker H-bond acceptor (β_s = 4.7). When the hydroxyl group in the Y-position was replaced by an amino group, the populations of the *D* conformer were seen to decrease in all of the solvents studied, indicating that the OH···arene interaction is stronger than the NH···arene interaction in these compounds.[28]

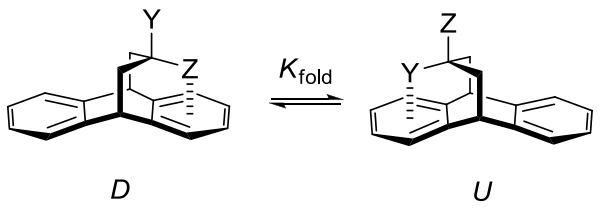

Z = OH, Y = H
Z = OH, Y = Me
Z = OH, Y = *n*-Bu
Z = OH, Y = CN
Z = OH, Y = C≡CH
Z = OMe, Y = Me
Z = OMe, Y = *n*-Bu

Z = O, Y = CH_2
Z = O, Y = $(CH_2)_2$
Z = OCH_2, Y = SCH_2
Z = F, Y = Me
Z = NH_2, Y = Me
Z = NH_2, Y = CN

Figure 7. Motherwell's molecular torsion balance for quantifying functional group···arene interactions in organic solvents.[27, 28]

Not all molecular balances reveal information about non-covalent interactions through changes in the position of a conformational equilibrium. Indeed, Elguero, Cornago and co-workers have used the position of tautomeric equilibria in pyrazole derivatives to investigate intramolecular NH···arene interactions (Figure 8).[29] At low concentrations, the tautomers are in slow exchange on the ^{1}H-NMR timescale in a range of deuterated solvents (chloroform, dichloromethane, dimethylsulfoxide and hexamethylphosphoramide). The barrier to tautomerisation decreases as the concentration of the pyrazole increases, presumably due to intermolecular association and proton exchange *via* the adjacent pyrazole ring nitrogen and NH groups. ^{1}H NMR showed a large shielding of the NH proton in tautomer 1 consistent with the NH···arene interaction shown. Tautomer 1 was >98% abundant when R = CF_3 in all solvents examined, which was attributed to the strengthening of polar NH···arene interaction by the strong electron-withdrawing effect of the CF_3 group.

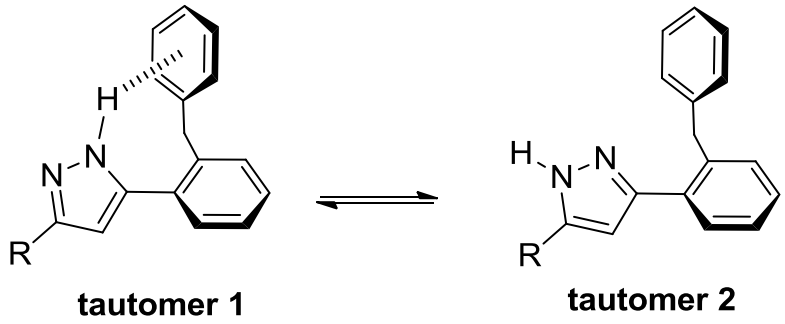

Figure 8. Polar NH···arene interactions have been quantified by using the tautomeric equilibria in pyrazoles when R = Me, CF_3 and Ph.[29]

Functional-group···arene interactions have also been studied in a more biological context using simple folding peptides in aqueous solution. Waters and co-workers used thermodynamic double-mutant cycles,[15] to quantify non-covalent interactions between the X^1 and X^2 side-chains in β-hairpin folds (Figure 9, left). This model system has been used to study cation···arene interactions between an aromatic tryptophan residue and cationic amine side-chains (Figure 9a).[30] Shielding of the protons in the lysine side-chain was observed by NMR spectroscopy due to close proximity of the tryptophan ring in the folded conformation. The chain length of the cationic side-chain was found to affect the interaction with tryptophan, and thus the stability of the β-hairpin fold. Shortening of the side-chain in the sequence: Lys > Orn > Dab decreased the favourability of the cation···arene interaction, with lysine having the optimal length for a diagonal interaction. The strength of this interaction and the stability of the β-hairpin were also seen to increase upon *N*-methylation of the lysine analogues.

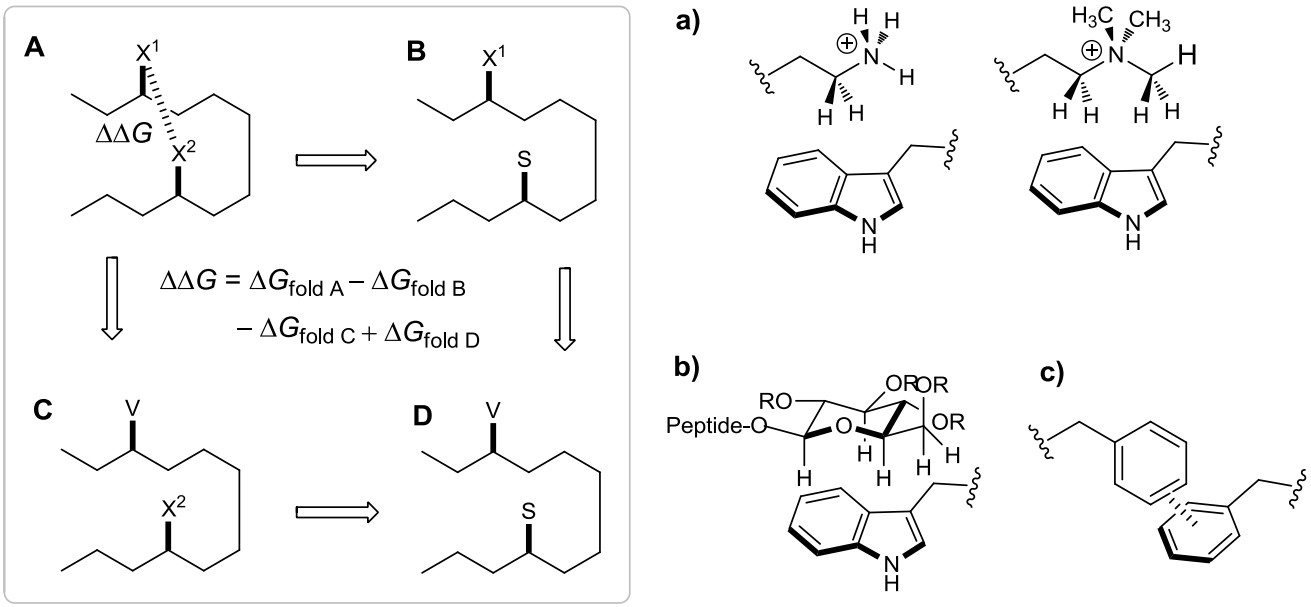

Figure 9. Example of a thermodynamic double-mutant cycle used by Waters and co-workers for the quantification of a range of arene···functional-group interactions in folded β-hairpin peptides.; a) cation···arene interactions, b) carbohydrate···arene interactions (R = H or Ac), and c) aromatic edge-to-face interactions. [30-33]

In addition, β-hairpin peptides have been used to quantify carbohydrate···arene interactions (Figure 9b).[31, 32] The carbohydrate protons are shifted upfield in the NMR spectra due to the close proximity to the aromatic tryptophan ring in the folded peptide. There was an insignificant change in the stability of the fold when the tryptophan indole side-chain was substituted for a 1-naphthyl or 2-naphthyl group. In contrast, replacing the tryptophan residue with the smaller aromatic amino acid, phenylalanine, decreased the stability of the peptide fold. Similar destabilisation was also observed upon substitution of the tryptophan residue for a non-aromatic cyclohexyl side-chain. A strong solvophobically driven interaction was only seen between tryptophan and fully acylated carbohydrates (Figure 9b, R = Ac) and not with the unprotected carbohydrates due to the high energetic penalty required to desolvate the unprotected hydroxyl groups. Strikingly, the carbohydrate···arene interaction was found to be stronger than the arene···arene interaction between two phenylalanine side-chains (Figure 9c), or the cation···arene interaction between tryptophan and lysine (Figure 9a).[31, 33]

Wilcox and co-workers have also studied alkyl···arene contacts using molecular torsion balances (Figure 10).[34, 36] Indeed, Wilcox was the first to coin the phrase ‘molecular torsion balance’, with the most recent studies building upon measurements published in 1994 (see Section 3.3).[34]

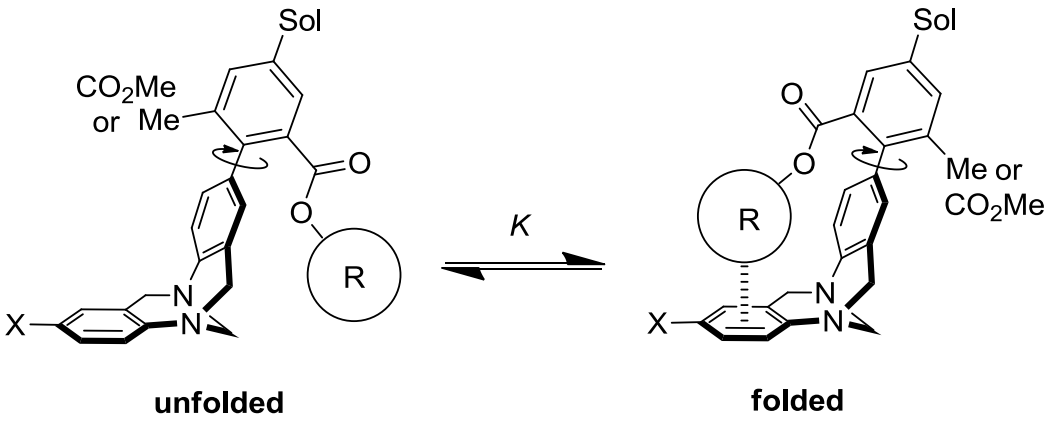

Figure 10. Molecular torsion balances designed by Wilcox and later used by others for measuring aromatic edge-to-face interactions in organic solvents (R = substituted phenyl rings), and alkyl···arene interactions (R = Me, *i*-Pr, *t*-Bu, cyclohexyl, 1-adamantyl, 2-adamantyl) in $CDCl_3$ (Sol = NO_2, H, NH_2) and D_2O (Sol = $NHCO(CH_2)_3COO^-K^+$).[10,-12, 34-39]

Like the triptycene balances discussed earlier, the folded and unfolded conformations in Wilcox's balance are visible as distinct signals in ^{1}H-NMR spectra. The two conformations arise from the hindered rotation about the biaryl bond. Deviation from a 1:1 ratio of states indicates the presence of a non-covalent interaction or solvent effect. When R = Me there is little or no preference for either conformation, as the methyl group is too far from the face aromatic ring to interact.[35] However, when R is replaced by a larger alkyl group the folded conformation is seen to dominate in both D_2O and $CDCl_3$. The balance is most folded in aqueous solution and when R = *i*-Pr, highlighting the importance of the hydrophobic effect and shape complementarity in non-covalent interactions.[34, 36]

3.3 Aromatic edge-to-face interactions

Aromatic edge-to-face interactions have received considerable attention from supramolecular chemists, partly due to their importance in stabilising the structure of proteins and peptides.[33, 40]

Wilcox and co-workers pioneered the use of molecular torsion balances for studying aromatic edge-to-face interactions (Figure 10).[34] By varying both the R-group with differently substituted phenyl rings, and the X-substituent on the 'face-ring', it was possible to systematically examine the effects of substituents on the folding free energy. Aromatic R-groups featuring electron-withdrawing groups such as CN, CF_3 and NO_2 shift the equilibrium towards the folded conformation, which can be explained by an increase in the electrostatic attraction between the partial positive charge of the edge of the aromatic ring with the electron-density of the aromatic face.[11, 12, 34, 38, 39] Other experiments involving variation of the X-substituents on the 'face-

ring' revealed a much more surprising result; the folding free energies of the torsion balances appeared to be insensitive to variation of the X-substituents in $CDCl_3$ when R was an unsubstituted phenyl ring.[35, 37-39] This observation led Wilcox to conclude that dispersion forces, and not electrostatic forces, dominate aromatic edge-to-face interactions in this system.[35] However, experimental work published by Ren in 1997, and Diederich in 2004 and 2008, revealed that the solvent has a significant influence on the folding behaviour of these molecules.[37-39] Particularly worthy of note was the observation that folding free energies when R = *p*-trifluoromethyl phenyl correlated linearly with Hammett substituent constants in both C_6D_6 and $CDCl_3$. This implies an important role for electrostatic effects in edge-to-face interactions, and contradicts Wilcox's earlier conclusions. Cockroft and Hunter used a simple solvation model to rationalise the apparent discrepancy (Figure 1, top).[10] The key point is that solvation of the face-ring competes with the edge-to-face aromatic interaction formed upon folding. Thus, when R is a phenyl ring with an electron-withdrawing substituent, the positively polarised edge of the aromatic ring outcompetes the solvation of the face ring by both chloroform and benzene and the folding free energies vary significantly as the electrostatic potential of the aromatic face is modulated by changing the X-substituents. In contrast, when R is an unsubstituted phenyl ring, the edge-to-face interaction formed in the folded conformation is similar in magnitude to the interaction between the face aromatic ring and the solvent (in $CDCl_3$ and C_6D_6), so the folding free energies change only slightly upon variation of the X-substituents on the face ring. The most obvious prediction made by this model is that benzene solvation should compete equally as well for the edge-to-face interaction as R = Ph, a result that was later confirmed experimentally by Diederich and co-workers.[12, 39]

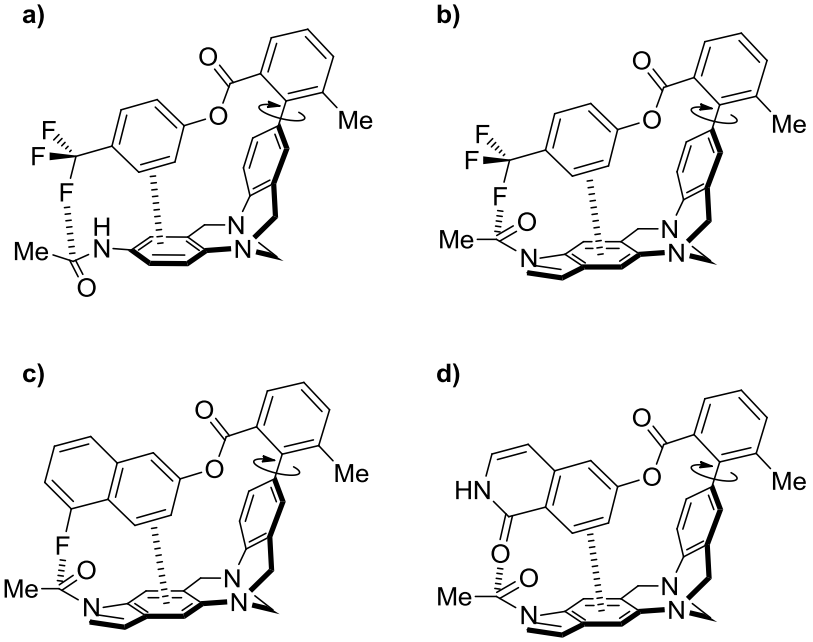

Figure 11. a)-c) Wilcox torsion balances synthesised by Diederich and co-workers for examining F···amide[38, 41] and d) carbonyl···amide interactions.[42]

Diederich has utilised the desirable edge-to-face geometry of the Wilcox torsion balance in combination with thermodynamic double-mutant cycles[15] to quantify C-F···carbonyl, and carbonyl···carbonyl interactions between orthogonally orientated aromatic substituents (Figure 11).[38, 41, 42]

Recently, Cozzi and co-workers studied the interaction of the face of a phenyl ring with both the edge of another phenyl ring, and the nitrogen of a pyridine ring using variable-temperature NMR experiments (Figure 12).[43] The barriers to topomeric flipping of the *meta*-substituted ring were increased upon fluorination of the face-ring, with the highest barrier being observed with the pyridine ring. The lowest barrier to flipping was observed with the benzene ring and the non-fluorinated face ring. Despite the appealing simplistic design of these molecules, calculated energy landscapes for the topomerisation process contained multiple transition states, highlighting the complexities involved in the interpretation of $\Delta G^{\ddagger}$ measurements. Rationalisation of the observed barriers to rotation was further convoluted because the energetics of the ground-state conformations and each of the transition states were modulated to different extents as the substituents were varied.

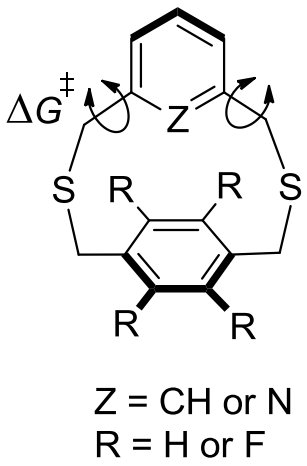

Figure 12. Topomeric model compounds designed by Cozzi to measure tilted edge-to-face aromatic interactions.[43]

3.4 Aromatic stacking interactions

Gellman and co-workers expanded on their earlier qualitative studies of aromatic stacking interactions (Figure 2a) by developing a series of folding molecules for quantifying aromatic interactions (Figure 13).[9, 44, 45] These compounds exist as two slowly interconverting conformers *via* rotation about with each other, but in the *E* conformation the aromatic rings can come into a stacked arrangement (as supported by

X-ray crystal structures). The conformer ratios of the compounds shown in Figs. 13a and 13b were similar in $CDCl_3$ solution, but were quite different in D_2O. This was attributed to the hydrophobic stabilisation of the *E* conformer, which minimises the solvent-exposed surface area of the apolar aromatic moieties (Figure 1, top). A derivative where one of the aromatic groups was replaced with a phenyl ring was seen to have similar folding ratios in both water and chloroform, presumably because the phenyl group does not reach far enough to interact with the naphthyl group (Figure 13b, Y = H). Thus, the contribution of the arene···arene interaction to the observed folding free energies could be quantified by subtracting the folding free energy of this reference compound from those observed in the other variations shown in Figs. 13a and 13b. The folded *E* configuration was favoured when nitrogen atoms were introduced into one or both of the aromatic rings, (Figure 13b, Y= pyridyl or pyrimidyl).[45] This observation cannot be attributed to the hydrophobic effect since the nitrogen heterocycles are less hydrophobic than the naphthyl group. Instead, these observations are consistent with the formation of electrostatically dominated edge-to-face aromatic contacts (see Section 3.3). Indeed, the stacked geometry is not enforced in these compounds, the terminal aromatic groups are free to rotate in solution, and the lowest energy conformation of the biaryl compounds employed are twisted propeller conformations. Furthermore, the *E/Z* ratios increased in-line with the positive polarisation of the aromatic edges induced by the addition of electronegative nitrogen atoms.

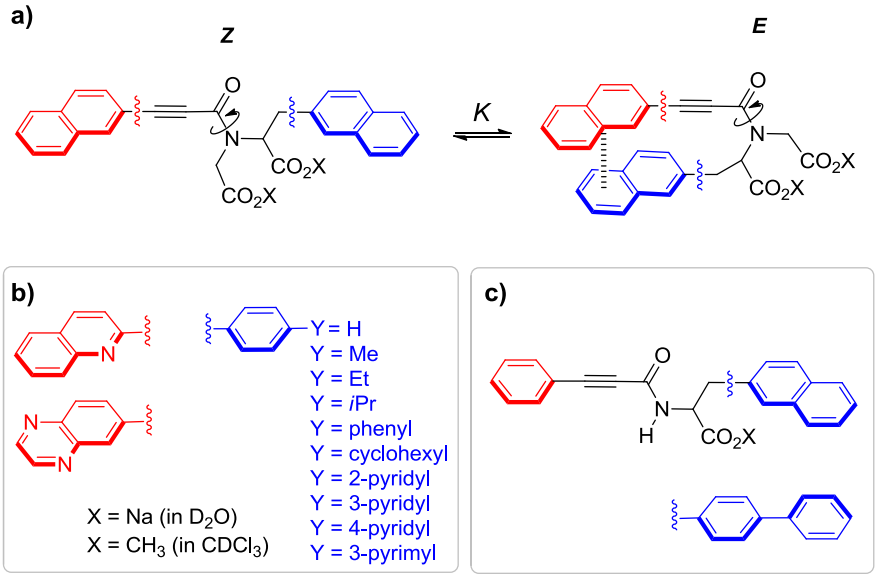

Figure 13. Folding molecules designed by Gellman for quantifying aromatic stacking interactions in D_2O and $CDCl_3$.[9, 44, 45]

Unlike tertiary amides, secondary amides typically exist predominantly in the *Z* conformation due to repulsive steric interactions between the substituents on the amide carbon and nitrogen atoms. Despite

this, the hydrophobic stacking of the aromatic groups in the secondary amides depicted in Figure 13c was substantial enough that significant populations of the *E* conformers could be observed in aqueous solution.[9]

Cozzi, Siegel and co-workers have investigated aromatic stacking interactions in a range of geometries by measuring the barrier to rotation ($\Delta G^{\ddagger}$) about biaryl bonds (Figure 14).[46-48] Parallel-offset stacking interactions were investigated by varying the X-substituent using the system shown in Figure 14a.[46] The barrier to rotation increased as the X-substituent became more electron-withdrawing, since this decreases repulsion between the rings and stabilises the stacked ground state. Linear relationships were observed between $\Delta G^{\ddagger}$ and the Hammett substituent constants, indicating that electrostatic effects dominate the system. The same trends were observed in the 1,8-diarylnaphthalene system (Figure 14b), where the aromatic groups are forced into a sterically strained stacked arrangement, but the changes in the barrier to rotation were larger than those observed in the off-set stacked system (Figure 14a). It was reasoned that the parallel-offset stacking interactions were less repulsive than parallel stacked interactions in these strained systems.[46] To further test the proposed electrostatic model, the successive addition of electronegative fluorine atoms to one of the rings in the strained stacked system (Figure 14b) was seen to increase the barrier to rotation.

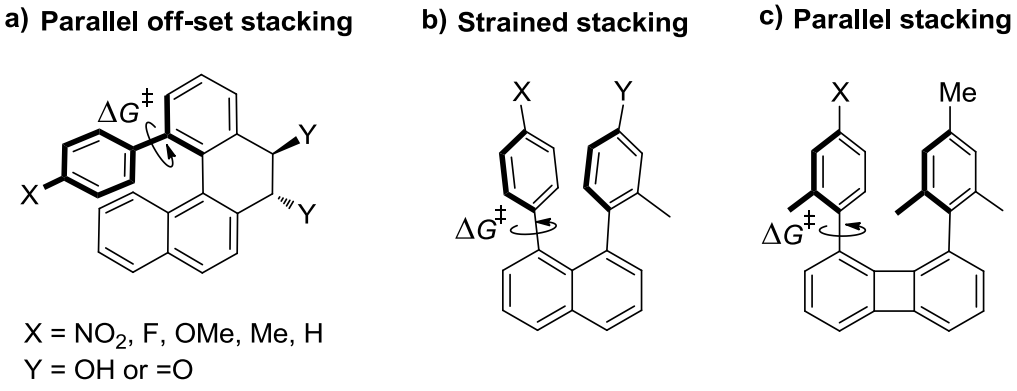

Figure 14. Model systems used by Cozzi and Siegel for studying aromatic stacking interactions in a variety of geometries. [46-48]

Cozzi and Siegel have recently expanded their research on aromatic interactions using a series of substituted 1,8-diarylbiphenylenes where the distance between the stacked aromatic groups was much closer to the equilibrium separation of stacking interactions observed in X-ray crystal structures (Figure 14c).[48] As seen in the earlier stacked systems, electron-donating X-substituents lowered the barrier to biaryl rotation, but these systems were much less sensitive to substituent effects. Surprisingly, the barrier

to rotation was insensitive to variation of the X-substituents when one of the rings was fluorinated. This was postulated to arise from a combination of van der Waals dispersive interactions and secondary interactions between the fluorine atoms and the X-substituents.

Zoltewicz and co-workers have also adopted strained 1,8-naphthalene derivatives to investigate a wide range of stacking interactions, but rather than measuring barriers to rotation, compounds which display *syn-anti* conformational isomerisation were studied (Figs. 15a-c).[49-54] The *syn* conformation was dominant for all of the compounds depicted in Figure 15a. The large upfield shielding of the ^{1}H-NMR methyl signals and the preference for the *syn* conformation can be attributed to the existence of favourable cation···arene and CH···arene interactions between the positively polarised methyl substituents of one ring and electron-rich naphthalene face of the other. Although solvent molecules cannot enter the space between the aromatic rings, they can easily interact with the edges of the aromatic rings and the substituents in the *anti* conformation. Polar solvents were found to stabilise the *anti* conformer most. Thus, changing the solvent from $CDCl_3$ to DMSO decreased the degree of stacking of the methylpyridinium moiety with naphthalene ring.[53] In contrast, when both aromatic rings were either electron-rich or electron-poor, electrostatic and steric repulsion dominated and the *anti* conformers were preferred (Figs. 15b and 15c).

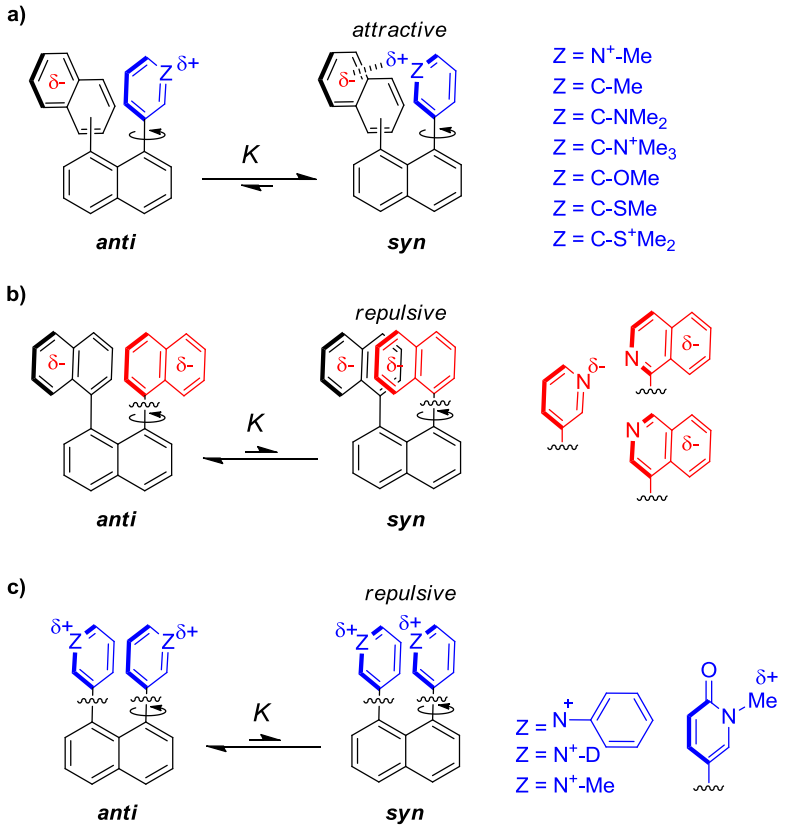

Figure 15. Model systems used by Zoltewicz for studying aromatic stacking interactions. [49-54]

In 2002, Waters examined substituent effects in offset stacking interactions using a related class of rotameric compounds (Figure 16a).[55] Whilst earlier studies had predominantly been performed in organic solvents, the polar nature of these cationic compounds enabled measurements to be obtained in aqueous solution. In line with the earlier findings of Siegel and co-workers, electron-withdrawing groups increased the barrier of rotation, which was also larger for *meta vs. para*-substituents. Further work examined how the interaction between a positively charged nitrogen and the face of another aromatic ring varied as the point of contact was changed (Figure 16b).[56] The offset-stacked geometry that places the *ortho* hydrogen of the pyridinium ring close to the phenyl ring was favoured. Computational models suggested that the two rings were splayed apart in the transition state and no stacking interaction was taking place. The compound with the nitrogen atom in the *ipso* position showed the largest $\Delta G^{\ddagger}$ followed by the *ortho*, *meta* and *para* analogues. Small changes to the barrier to rotation were observed upon alkylation of the nitrogen atom. This indicated that specific $^{+}$NH···π or $^{+}$NMe···π interactions were not dominant in the system, which was consistent with the fact that the positive charge of the pyridinium ion is delocalised over the entire aromatic surface.

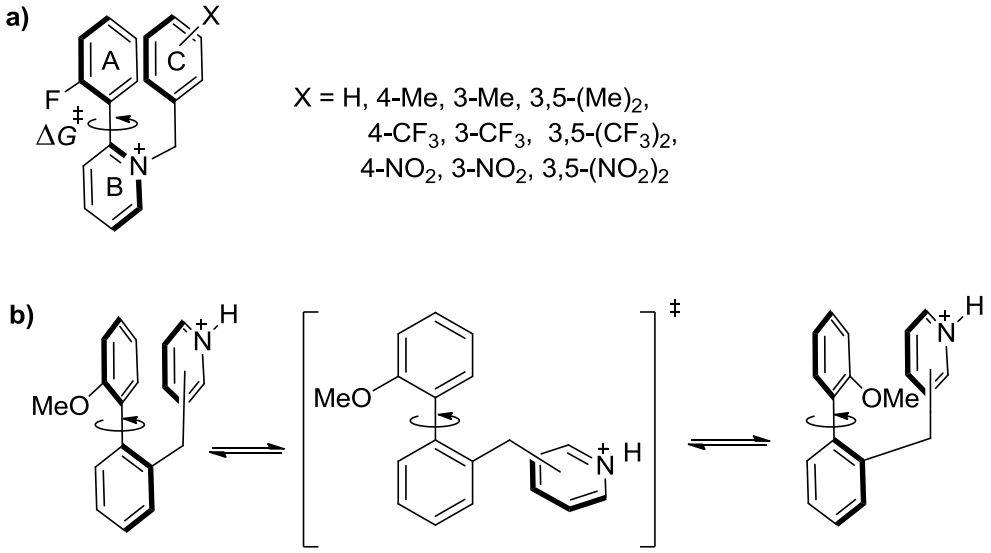

Figure 16. Torsion balances designed by Waters to measure aromatic cation···arene interactions in aqueous solution.[55, 56]

Shimizu and co-workers recently synthesised a series of molecular balances for quantifying aromatic stacking interactions (Figure 17).[57] In the folded conformation, only a face-to-face aromatic stacking interaction can occur because the distance between the two arenes is too small to accommodate an edge-to-face interaction. The compounds with the phenanthrene or pyrene 'shelves' were found to have higher

folded/unfolded ratios than the compound with the smaller phenyl shelf. The phenyl platform is too small to facilitate an aromatic stacking interaction with the phenyl ether arm, thus this compound was used as a control compound to measure secondary interactions. The free energy of the interaction was measured in different solvents, with more polar solvents shifting the equilibrium towards the folded conformation, consistent with solvophobically driven folding (Fig 1, top left).

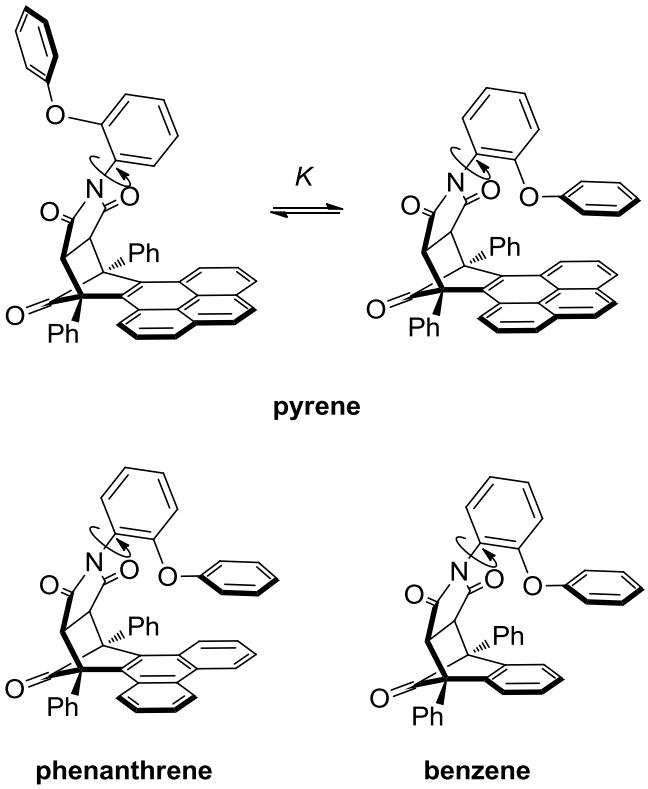

Figure 17. Molecular torsion balances designed by Shimizu for quantifying aromatic stacking interactions.[57]

Most recently, Shimizu and co-workers synthesised a new torsion balance for quantifying interactions between extended aromatic face-to-face contacts (Figure 18).[58] The high barrier to *syn*/*anti* interconversion (113 kJ mol^{-1}) in these compounds meant that the *anti* atropoisomers could be isolated and the X-ray crystal structures determined. These solid-state snapshots showed that the aromatic groups were stacked on either face of the naphthalene diimide as depicted on the right-hand side of Figure 18. The folding free energies increased in an upwardly curving trend as the area of contact between the interacting aromatic groups was increased. This could be attributed to an increase in dispersion interactions as the size of the aromatic contacts increase, or alternatively may be the result of an entropic co-operative effect.[59] The folding free energies did not change significantly upon changing the solvent from tetrachloroethane to dimethylsulfoxide.

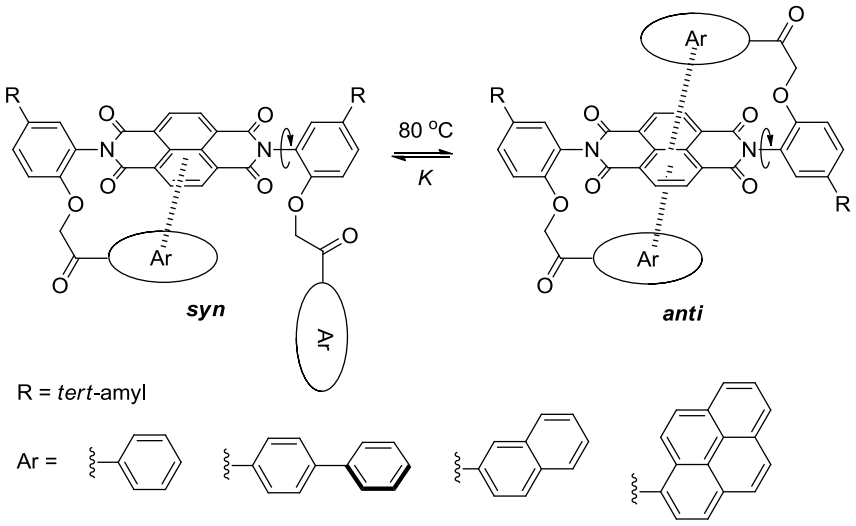

Figure 18. Molecular torsion balances synthesised by Shimizu and co-workers for quantifying aromatic stacking interactions between the central electron-poor naphthalene diimide surface and a range of aromatic groups.[58]

Building on the seminal work of Ōki, Gung and co-workers have adopted triptycenes in the study of substituent effects on aromatic stacking interactions in both the face-to-face and offset-stacked geometries in organic solvents (Figs. 19-21).[60-62] A non-linear relationship between interaction energies and Hammett *para*-substituent constants was reported and attributed to charge-transfer interactions. Correlating these results against calculated ring-centre electrostatic potentials (Figure 20), or Hammett constants from another source[63] removes much of the curvature in the trends.

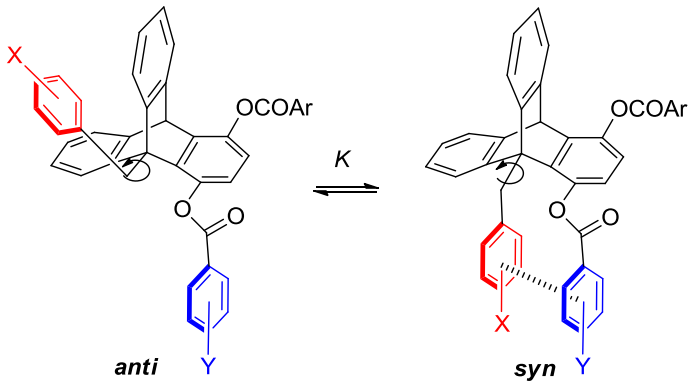

Figure 19. 1,9-disubstituted triptycenes used by Gung and co-workers for quantifying offset aromatic stacking interactions.[60-62]

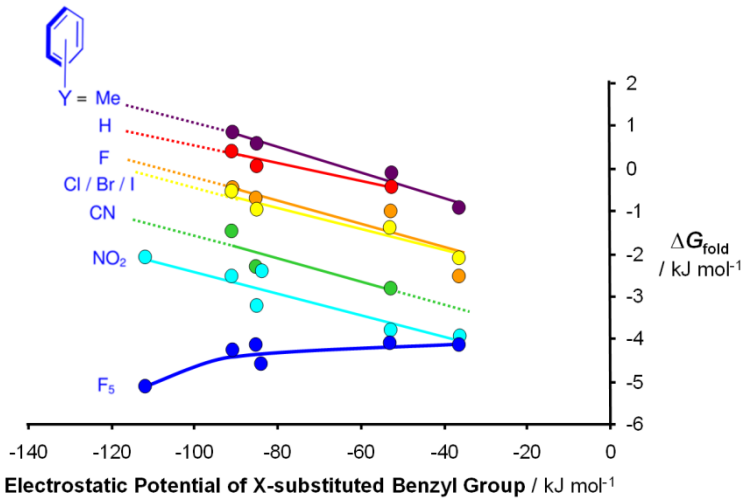

Figure 20. Experimental folding free energies (ΔG)[60, 61] plotted against the DFT/B3LYP-6-31G*-calculated electrostatic surface potentials taken above the ring centroids of the X-substituted aromatic ring for the triptycene balances depicted in Figure 19. Values were measured in $CDCl_3$ at –40 °C, and the NO_2-, Cl-, I- and perfluoro-substituted phenyl ester groups were measured at –15 °C. Data for the Cl, Br and I-substituted phenyl ester series were very similar - as would be expected from calculated electrostatic potentials - despite being obtained at different temperatures (only the chlorophenyl ester series are plotted for purposes of clarity). The *syn*/*anti* ratios of some nitrophenyl ester compounds were measured at both –15 °C and –40 °C and the interaction trends are very similar.

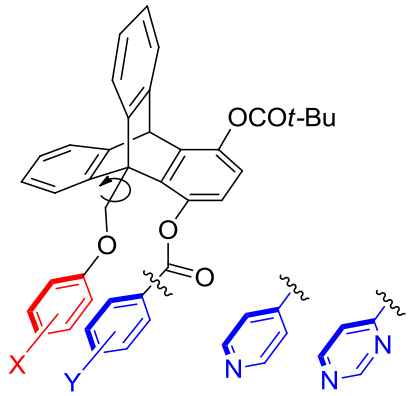

X = *p*-NMe_2, *p*-OMe, *p*-Me, H, *p*-NO_2, 3,5-diMe, 3,4,5-triMe

Y = *p*-OMe, H, *p*-NO_2, *p*-CN, *p*-Me, 3,5-diMe, 3,4,5-triMe, *p*-F, 2,6-diF, 2,4,6-triF, 2,3,5,6-tetraF, pentaF

Figure 21. 1,9-disubstituted triptycenes used by Gung and co-workers for quantifying near-sandwich stacked aromatic interactions. Note the additional oxygen atom adjacent to the X-substituted ring compared to the compounds shown in Figure 19.[66, 67]

However, curvature does remain for the pentafluorophenyl data series (dark blue points in Figure 20), which may be consistent with a role for charge-transfer interactions between the most electron-deficient and electron-rich aromatic rings. Just as Cozzi, Siegel[47] and Hunter[64, 65] have found in other stacked systems, the gradient of the stacking interaction trend in Figure 20 is inverted when an electron-rich aromatic group is replaced by an electron-poor pentafluorophenyl group.

Furthermore, the *syn*/*anti* ratios for the compounds were reduced in bromobenzene-d_5 compared to $CDCl_3$, in accordance with increased solvent competition. In the most recent work, the stacking interaction was found to be more favourable when a methyl group was installed in the *ortho*-position *vs*. the *para*-position on the X-substituted ring.[62]

Gung went on to investigate near-perfect face-to-face stacking interactions by inserting an oxygen atom into the linker attached to the X-substituted arene (Figure 21).[66] Again, interactions were found to be repulsive with electron-rich monosubstituted rings, but attractive when an electron-poor arene ring was involved. A linear correlation of the folding free energy with the number of fluorine atoms attached to the phenyl ester, indicated that the more electron-deficient the system, the more attractive the interaction. The *syn* conformation became dominant when the Y-substituted ring was replaced by a pyridine or pyrimidine ring (Figure 21).[67] The most favourable interaction was observed when an electron-rich X-substituted benzene ring interacted with the electron-poor pyrimidine ring, mirroring the results obtained by Gellman (Figure 13b). It should be noted that the stacking interaction is not enforced in Gung's system and the additional oxygen atom may provide enough conformational flexibility to accommodate an edge-to-face aromatic contact in solution.

Conclusions

The study of non-covalent interactions leads to a greater understanding of the principles governing the behaviour of chemical and biological systems. Molecular balances and folding molecules offer several advantages that make them excellent tools for expanding our understanding of non-covalent interactions:

- Simple model compounds overcome the difficulties of studying complicated biological systems.
- Synthetic modifications allow systematic variation of functional groups and interaction geometries to test current theories of molecular interactions.
- Very weak, repulsive, or entropically disfavoured interactions can be measured using conformationally well-designed compounds.

Several classes of molecular balances have been developed for the quantitative study of non-covalent interactions to date. Aromatic interactions have been particularly well-studied, and the scope of the

approach continues to expand. The subtle interplay of numerous factors contributing to non-covalent interactions probably limits the transferability of absolute interaction energies measured using molecular balances. However, despite this caveat, molecular balances are able to provide insights into the physicochemical origins of molecular recognition; they have already contributed to the development of empirical solvation models, and future investigations have the potential to reveal previously overlooked or unidentified phenomena.

Refrences

[1] D. B. Amabilino and J. F. Stoddart, *Chem. Rev.,* 1995, **95**, 2725-2829.

[2] J. Clayden, *Chem. Soc. Rev.* 2009, **38**, 817-829.

[3] J. M. Lehn, *Science*, 2002, **295**, 2400-2403.

[4] S. Deechongkit, H. Nguyen, E. T. Powers, P. E. Dawson, M. Gruebele and J. W. Kelly, *Nature*, 2004, **430**, 101-105.

[5] A. T. Krueger and E. T. Kool, *Curr. Opin. Chem. Biol.*, 2007, **11**, 588-594.

[6] E. T. Kool and M. L. Waters, *Nat. Chem. Biol.*, 2006, **3**, 70-73.

[7] H. J. Schneider, *Angew. Chem. Int. Ed.*, 2009, **48**, 3924-3977.

[8] J. Sandström, *Dynamic NMR Spectroscopy*, Academic Press, London, UK, 1982.

[9] R. R. Gardner, S. L. McKay and S. H. Gellman, *Org. Lett.*, 2000, **2**, 2335-2338.

[10] M. Nakamura, K. N. Houk, *Org. Lett.* 1999, **1**, 2049-2051.

[11] S. L. Cockroft and C. A. Hunter, *Chem. Commun.*, 2006, 3806-3808.

[12] S. L. Cockroft and C. A. Hunter, *Chem. Commun.*, 2009, 3961- 3963.

[13] L. F. Newcomb and S. H. Gellman, *J. Am. Chem. Soc.*, 1994, **116**, 4993-4994.

[14] S. Sankararaman, G. Venkataramana and B. Varghese, *J. Org. Chem.*, 2008, **73**, 2404-2407.

[15] S. L. Cockroft and C. A. Hunter, *Chem. Soc. Rev.*, 2007, **36**, 172-188.

[16] M. Nakamura, M. Ōki, H. Nakanishi and O. Yamamoto, *Bull. Chem. Soc. Jpn.*, 1974, **47**, 2415-2419.

[17] M. Ōki, *Acc. Chem. Res.*, 1990, **23**, 351-356.

[18] M. Ōki, *Angew. Chem. Int. Ed. Eng.*, 1976, **15**, 87-93.

[19] C. A. Hunter, *Angew. Chem. Int. Ed.*, 2004, **43**, 5310-5324.

[20] M. Ōki, G. Izumi, G. Yamamoto and N. Nakamura, *Chem. Lett.*, 1980, 213-216.

[21] G. Izumi, G. Yamamoto and M. Ōki, *Chem. Lett.*, 1980, 969-972.

[22] M. Ōki, G. Izumi, G. Yamamoto and N. Nakamura, *Bull. Chem. Soc. Jpn.*, 1982, **55**, 159-166.

[23] Y. Tamura, G. Yamamoto and M. Ōki, *Chem. Lett.*, 1986, 1619-1622.

[24] Y. Tamura, G. Yamamoto and M. Ōki, *Bull. Chem. Soc. Jpn.*, 1987, **60**, 1781-1788.

[25] B. W. Gung, X. Xue and H. J. Reich, *J. Org. Chem.*, 2005, **70**, 7232-7237.

[26] B. W. Gung, Y. Zou, Z. Xu, J. C. Amicangelo, D. G. Irwin, S. Ma and H. C. Zhou, *J. Org. Chem.*, 2008, **73**, 689-693.

[27] W. B. Motherwell, J. Moise, A. E. Aliev, M. Nic, S. J. Coles, P. N. Horton, M. B. Hursthouse, G. Chessari, C. A. Hunter and J. G. Vinter, *Angew. Chem. Int. Ed.*, 2007, **46**, 7823-7826.

[28] A. E. Aliev, J. Moise, W. B. Motherwell, M. Nic, D. Courtier-Murias and D. A. Tocher, *Phys. Chem. Chem. Phys.*, 2009, **11**, 97-100.

[29] P. Cornago, R. M. Claramunt, L. Bouissane and J. Elguero, *Tetrahedron*, 2008, **64**, 3667-3673.

[30] R. M. Hughes, M. L. Benshoff and M. L. Waters, *Chem. -Eur. J.*, 2007, **13**, 5753-5764.

[31] S. E. Kiehna, Z. R. Laughrey and M. L. Waters, *Chem. Commun.*, 2007, 4026-4028.

[32] Z. R. Laughrey, S. E. Kiehna, A. J. Riemen and M. L. Waters, *J. Am. Chem. Soc.*, 2008, **130**, 14625-14633.

[33] C. D. Tatko and M. L. Waters, *J. Am. Chem. Soc.*, 2002, **124**, 9372-9373.

[34] S. Paliwal, S. Geib and C. S. Wilcox, *J. Am. Chem. Soc.*, 1994, **116**, 4497-4498.

[35] E. Kim, S. Paliwal and C. S. Wilcox, *J. Am. Chem. Soc.*, 1998, **120**, 11192-11193.

[36] B. Bhayana and C. S. Wilcox, *Angew. Chem, Int. Ed.*, 2007, **46**, 6833-6836.

[37] T. Ren, Y. Jin, K. S. Kim and D. H. Kim, *J. Biomol. Struct. Dyn.*, 1997, **15**, 401-405.

[38] F. Hof, D. M. Scofield, W. B. Schweizer and F. Diederich, *Angew. Chem. Int. Ed.,* 2004, **43**, 5056-5059.

[39] F. R. Fischer, W. B. Schweizer and F. Diederich, *Chem. Commun.*, 2008, 4031-4033.

[40] S. K. Burley and G. A. Petsko, *Science*, 1985, **229**, 23-28.

[41] F. R. Fischer, W. B. Schweizer and F. Diederich, *Angew. Chem. Int. Ed.*, 2007, **46**, 8270-8273.

[42] F. R. Fischer, P. A. Wood, F. H. Allen and F. Diederich, *Proc. Natl. Acad. Sci. U. S. A.,* 2008, **105**, 17290-17294.

[43] R. Annunziata, M. Benaglia, F. Cozzi and A. Mazzanti, *Chem. -Eur. J.*, 2009, **15**, 4373-4381.

[44] R. R. Gardner, L. A. Christianson and S. H. Gellman, *J. Am. Chem. Soc.*, 1997, **119**, 5041-5042.

[45] S. L. McKay, B. Haptonstall and S. H. Gellman, *J. Am. Chem. Soc.*, 2001, **123**, 1244-1245.

[46] F. Cozzi, R. Annunziata, M. Benaglia, M. Cinquini, L. Raimondi, K. K. Baldridge and J. S. Siegel, *Org. Biomol. Chem.*, 2003, **1**, 157-162.

[47] F. Cozzi and J. S. Siegel, *Pure Appl. Chem.*, 1995, **67**, 683-689.

[48] F. Cozzi, R. Annunziata, M. Benaglia, K. K. Baldridge, G. Aguirre, J. Estrada, Y. Sritana-Anant and J. S. Siegel, *Phys. Chem. Chem. Phys.*, 2008, **10**, 2686-2694.

[49] J. A. Zoltewicz, N. M. Maier and W. M. F. Fabian, *J. Org. Chem.*, 1996, **61**, 7018-7021.

[50] J. A. Zoltewicz, N. M. Maier and W. M. F. Fabian, *J. Org. Chem.*, 1997, **62**, 2763-2766.

[51] J. A. Zoltewicz, N. M. Maier and W. M. F. Fabian, *J. Org. Chem.*, 1997, **62**, 3215-3219.

[52] J. A. Zoltewicz, N. M. Maier, S. Lavieri, I. Ghiviriga, K. A. Abboud and W. M. F. Fabian, *Tetrahedron*, 1997, **53**, 5379-5388.

[53] J. A. Zoltewicz, N. M. Maier and W. M. F. Fabian, *J. Org. Chem.*, 1998, **63**, 4985-4990.

[54] S. Lavieri and J. A. Zoltewicz, *J. Org. Chem.*, 2001, **66**, 7227-7230.

[55] M. J. Rashkin and M. L. Waters, *J. Am. Chem. Soc.*, 2002, **124**, 1860-1861.

[56] M. J. Rashkin, R. M. Hughes, N. T. Calloway and M. L. Waters, *J. Am. Chem. Soc.*, 2004, **126**, 13320-13325.

[57] W. R. Carroll, P. Pellechia and K. D. Shimizu, *Org. Lett.*, 2008, **10**, 3547-3550.

[58] Y. S. Chong, W. R. Carroll, W. G. Burns, M. D. Smith and K. D. Shimizu, *Chem. -Eur. J.*, 2009, **15**, 9117-9126.

[59] C. A. Hunter and H. L. Anderson, *Angew. Chem. Int. Ed.*, 2009, **48**, 7488-7499.

[60] B. W. Gung, X. Xue and H. J. Reich, *J. Org. Chem.,* 2005, **70**, 3641-3644.

[61] B. W. Gung, M. Patel and X. Xue, *J. Org. Chem.*, 2005, **70**, 10532-10537.

[62] B. W. Gung, B. U. Emenike, C. N. Alverez, J. Rakovan, K. Kirschbaum and N. Jain, *Tetrahedron Lett.*, 2010, **51**, 1648-1650.

[63] C. Hansch, A. Leo and R. W. Taft, *Chem. Rev.,* 1991, **91**, 165-195.

[64] S. L. Cockroft, J. Perkins, C. Zonta, H. Adams, S. E. Spey, C. M. Low, J. G. Vinter, K. R. Lawson, C. J. Urch and C. A. Hunter, *Org. Biomol. Chem.*, 2007, **5**, 1062-1080.

[65] S. L. Cockroft, C. A. Hunter, K. R. Lawson, J. Perkins and C. J. Urch, *J. Am. Chem. Soc.*, 2005, **127**, 8594-8595.

[66] B. W. Gung, X. Xue and Y. Zou, *J. Org. Chem.*, 2007, **72**, 2469-2475.

[67] B. W. Gung, F. Wekesa and C. L. Barnes, *J. Org. Chem.*, 2008, **73**, 1803-1808.